

Optical selection rules for the quantum transitions from the ground state of the crystal to the superposition states of the two-dimensional magnetoexcitons

S. A. Moskalenko^a, I. V. Podlesny^a, I. A. Zubac^a, B. V. Novikov^b

^aInstitute of Applied Physics, 5, Academiei str., MD-2028, Chisinau, Republic of Moldova

^bDepartment of Solid State Physics, Institute of Physics, St. Petersburg State University, 1, Ulyanovskaya str., Petrodvorets, 198504, St. Petersburg, Russia

The band structure of the dichalcogenide monolayers was described in the Ref¹. This type of monolayers happens to be direct band gap semiconductors with minimal direct band gaps in the corner points \vec{K} and $-\vec{K}$ of the hexagonal Brillouin zone as is represented in the Figure 1. There are two valleys \vec{K} and $-\vec{K}$, where the valence electrons effectuate the direct optical quantum transitions in the conduction bands conserving their spin projections. Due to the symmetry of the Hamiltonian as regards the time inversion in the structures without center of inversion, the Kramers theorem establishes that the energy of electron with spin up in the valley \vec{K} equals to the energy of the electron with spin down in the valley $-\vec{K}$. This property is reflected in the Figure 1. The direct optical quantum transitions take place with the participation of the photons with different circular polarizations. The bare Wannier-Mott excitons appearing in \vec{K} and $-\vec{K}$ valleys due to the direct Coulomb electron-hole interactions have the same energies of their binding and creation. Two degenerate valley exciton states can be characterized by the valley pseudospin projections.

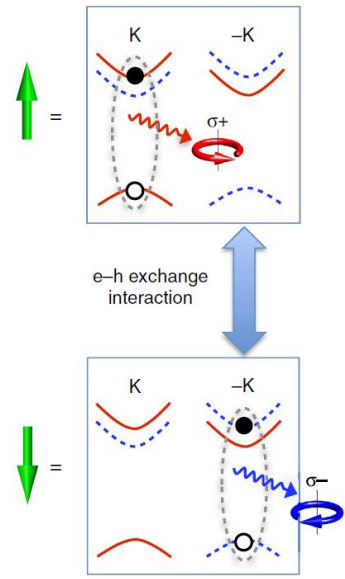


Figure 1. Valley-orbit coupled exciton X_0 . Valley pseudospin up and down configurations of X_0 . The figure is reproduced from the Ref¹.

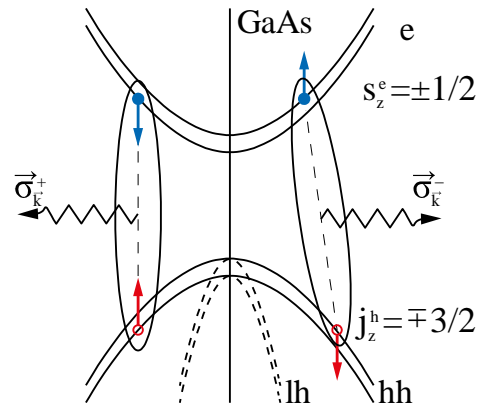


Figure 2. The band structure of GaAs crystal. The figure is reproduced from the Ref⁵.

The band structure of the GaAs quantum wells (QWs) in the absence of the external perpendicular magnetic field is represented in the Figure 2. The conduction electrons have the spin projections $s_z^e = \pm 1/2$ and the heavy holes have the full angular momentum projections $j_z^h = \pm 3/2$. The total angular momentum projection of the e-h pair $F = s_z^e + j_z^h$ is a quantum number characterizing the states of the e-h pairs and of the excitons. It has four possible values $F = \pm 1, \pm 2$. Two exciton states with $F = \pm 1$ are represented in the Figure 2. They can emit photons with different circular polarizations. As in the case of the TMDCs in the case GaAs QWs there are two bare exciton degenerate states interacting with photons of different circular polarizations. The strong perpendicular magnetic field leads to the Landau quantization of the orbital motions and to formation of discrete energy levels of electrons and holes separately. Under the influence of the Lorentz force the magnetoexciton with in-plane wave vector \vec{k}_{\parallel} looks as an electric dipole as is

demonstrated in Figure 3. The binding energy and the ionization potential are determined by the direct Coulomb e-h interaction. The arm of the dipole is proportional to the center-of-mass wave vector but perpendicular to it. In spite of the change of the orbital structure of the magnetoexciton as compared to the Wannier-Mott exciton with hydrogen atom-type structure, the spin structure of the magnetoexciton remains the same as in the absence of the magnetic field up till the Rashba spin-orbit coupling (RSOC) is not taken into account. A new property of the 2D magnetoexciton is the interdependence between the center-of-mass and the relative e-h motions induced by the action of the Lorentz force. This interdependence happens to play an important role promoting to the formation of the Dirac cone dispersion law under the influence of the exchange e-h Coulomb interaction.

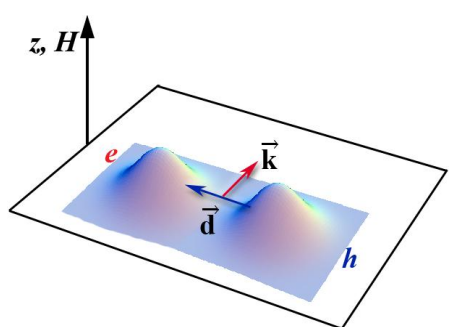


Figure 3. The electric-dipole model of the 2D magnetoexciton with the wave vector \vec{k} and with the arm of the electric dipole moment \vec{d} . The figure is reproduced from the Ref².

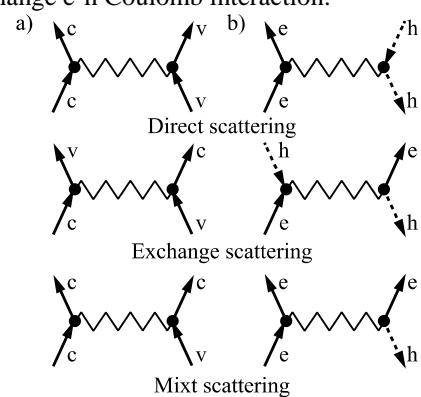


Figure 4. The electron-hole Coulomb scattering processes: a) in two-band representation; and b) in electron-hole description. The figure is reproduced from the Ref².

The diagrams representing the direct, exchange and mixed e-h Coulomb interactions are shown in the Figure 4. During the direct Coulomb scattering the particles are moving separately without changing of their origins. In the exchange scattering process the e-h pairs are created and annihilated. In the case of the valley excitons in the TMDCs such processes can take place with the electron from one valley and with the hole from another valley, what can lead to the interdependence between the center-of-mass and the relative e-h motions even in the absence of an external perpendicular magnetic field. The exchange e-h Coulomb interaction in both cases removes the degeneracy of the bare exciton states and leads to the formation of their coherent superposition states with well-defined coefficients of the linear combinations. Such superposition states in the case of two valley exciton states were demonstrated in the Ref¹. One of them has the Dirac cone dispersion law, whereas the another state has a Kirgiz hat-type dispersion law with minimum energy on the circle formed by the in-plane wave vectors. In the case of the 2D magnetoexcitons the superposition states are described by the next formulas

$$|\Psi_0^\pm\rangle = c_1^\pm \left[|\Psi_{ex}(-1; \vec{k}_{\parallel})\rangle \pm e^{-2i\varphi} |\Psi_{ex}(1; \vec{k}_{\parallel})\rangle \right], \quad E_{ex}^+(\vec{k}_{\parallel}) = E_{ex}^0(\vec{k}_{\parallel}) + \varepsilon_0 + I_1 \sqrt{2/\pi} \left| \frac{\rho_{c-v}}{l_0} \right|^2 e^{-\frac{|\vec{k}_{\parallel}|^2 l_0^2}{2}} |\vec{k}_{\parallel}| l_0,$$

$$E_{ex}^-(\vec{k}_{\parallel}) = E_{ex}^0(\vec{k}_{\parallel}) + \varepsilon_0; \quad \varepsilon_0 = -\frac{1}{2} I_1 \left| \frac{\rho_{c-v}}{l_0} \right|^2; \quad l_0^2 = \frac{\hbar c}{eB}, \quad E_{ex}^0(\vec{k}_{\parallel}) = -I_1 \cdot e^{-\frac{|\vec{k}_{\parallel}|^2 l_0^2}{4}} I_0 \left(\frac{|\vec{k}_{\parallel}|^2 l_0^2}{4} \right); \quad I_1 = \frac{e^2}{\varepsilon_0 l_0} \sqrt{\frac{\pi}{2}}.$$

The bare magnetoexciton states are determined by the quantum numbers $F = \pm 1$ in the way $|\Psi_{ex}(-1; \vec{k}_{\parallel})\rangle$ and $|\Psi_{ex}(1; \vec{k}_{\parallel})\rangle$, whereas the superposition states are denoted as $|\Psi_0^\pm\rangle$. One can see looking to the Figure 5 that the symmetric superposition state $|\Psi_0^+\rangle$

acquires a linear dispersion law in the range of the in-plane wave vectors $\vec{k}_{\parallel} l_0 < 1$, where l_0 is the magnetic length. The asymmetric superposition state $|\Psi_0^-\rangle$ remains with the same dispersion law as the bare magnetoexciton states.

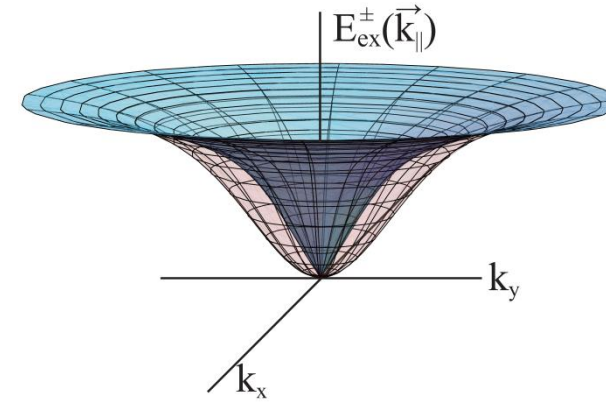


Figure 5. The branches of 2D bright magnetoexciton in two superposition states with and without Dirac cone dispersion law. The figure is reproduced from the Ref².

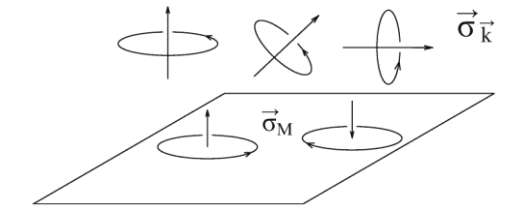


Figure 6. The circular polarizations of the photons and of the 2D excitons. The geometric selection rules are determined by the factors $|\langle \vec{\sigma}_K^\pm, \vec{\sigma}_M^\pm \rangle|^2$. The figure is reproduced from the Ref⁵.

As one can see looking at the Figure 6, the photons are propagating in any arbitrary directions of the 3D space, being characterized by the circular polarizations $\vec{\sigma}_K^\pm$. The 2D magnetoexcitons are located on the 2D plane of the layer. They are characterized by the quantum numbers $F = \pm 1$, what is equivalent to the circular polarization $\vec{\sigma}_M = (1/\sqrt{2})(\vec{a}_1 \pm i\vec{a}_2)$ with $F = M = \pm 1$. Here \vec{a}_1 and \vec{a}_2 are the in-plane unit vectors. The selection rules of the quantum transitions from the ground state of the crystal to the superposition states depend essentially on the quantum numbers n_e and n_h of the electron and of the hole Landau quantization levels. In the lowest Landau levels (LLs) approximation, when only the lowest numbers $n_e = n_h = 0$ are taken into account, the geometric selection rules depend on the scalar products $(\vec{\sigma}_K^\pm \cdot \vec{\sigma}_M^\pm)$ in their different combinations. It was shown² that the both superposition states are dipole active in the both circular polarizations. But in the case of symmetric state the probability of the quantum transition depends on the direction of the light propagation as regards the semiconductor layer. It has the dependence proportional to $k_z^2/|\vec{k}|^2$, where $\vec{k} = \vec{a}_3 k_z + \vec{k}_{\parallel}$, and \vec{a}_3 is the unit vector oriented perpendicularly to the layer surface. It is maximal in the Faraday geometry with light wave vector \vec{k} perpendicular to the surface of the layer, and vanishes in the Voigt geometry with the light propagation along to layer surface. Such dependence on the light wave vector projection k_z does not mean the appearance of the quadrupole quantum transition. It would be characterized by the quadratic dependence on the magnetoexciton in-plane wave vector \vec{k}_{\parallel} and would be looking as $|\vec{k}_{\parallel}|^2 l_0^2$. In the case of the asymmetric superposition state the probability of the quantum transition does not depend at all on the direction of the light propagation. These results are demonstrated in the Figure 7.

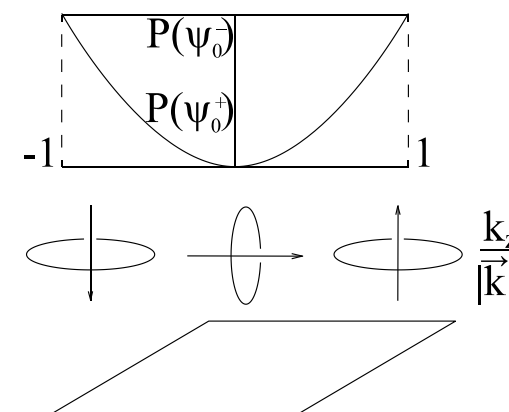


Figure 7. The selection rules of the quantum transitions in both circular polarizations from the ground state of the crystal to the superposition magnetoexciton states $|\Psi_0^\pm(\vec{k}_{\parallel})\rangle$. The figure is reproduced from the Ref².

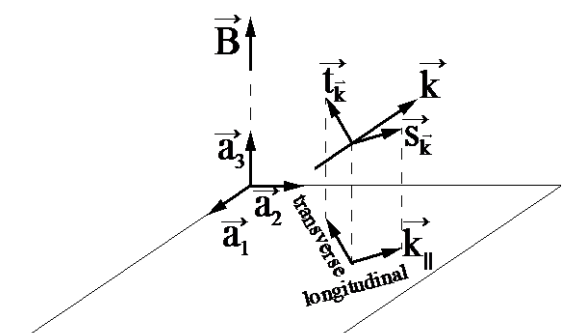


Figure 8. The selection rules of the quantum transitions in two linear polarizations.

The probability of the quantum transitions depend on the projections of the linear polarization vector \vec{s}_k and \vec{t}_k on the plane of the layer, especially whether they are longitudinal or transverse as regards the exciton in-plane wave vector \vec{k}_{\parallel} . The symmetric superposition state is dipole active in the linear polarization \vec{s}_k with longitudinal projection and is forbidden in the linear light polarization \vec{t}_k with transverse projection. As in the case of the circular polarizations the probability of quantum transition is proportional to $k_z^2/|\vec{k}|^2$. The asymmetric superposition state is dipole active in the linear polarization \vec{t}_k with transverse projection, is forbidden in the \vec{s}_k polarization and does not depend on the light orientation. The dependence of the probabilities of the quantum transitions in the exciton states of the TMDCs monolayers under the influence of the linearly polarized light also depend on the projections of the polarization vectors on the surface of the monolayers, as in the case of the 2D magnetoexcitons.

References

- [1] Hongyi, Y., Gui-Bin, L., Pu, G., Xiaodong, X. and Wang, Y., "Dirac cones and Dirac saddle points of bright excitons in monolayer transition metal dichalcogenides", Nature Commun. 5, 3876 (2014).
- [2] Moskalenko, S. A., Podlesny, I. V., Zubac, I. A. and Novikov, B. V., "Two-dimensional magnetoexciton superposition states with Dirac cone dispersion law and quantum interference effects in optical transitions", Solid State Commun. 312, 113714 (2020).
- [3] Moskalenko, S. A., [Vvedenie v teoriyu eksitonov bol'soi plotnosti], Isdatelstvo Stiintsa, Chisinau, 56-59 (1983) (in Russian).
- [4] Moskalenko, S. A., Podlesny, I. V., Zubac, I. A. and Novikov, B. V., "Superposition States of the Two-Dimensional Magnetoexciton with Dirac Cone Dispersion Law and Quantum Interference Effects in Optical Transitions", IFMBE Proc. 77, 13-17 (2020).
- [5] Moskalenko, S. A., Podlesny, I. V. and Zubac, I. A., "Two-dimensional exciton superposition states with Dirac cone dispersion laws," Mold. J. Phys. Sci. 18(1-4), 5-12 (2019).
- [6] Landau, L. D. and Lifshitz, E. M., [Quantum Mechanics Non-Relativistic Theory. Volume 3 of Course of Theoretical Physics. Translated from the Russian by J.B. Sykes and J.S. Bell. Second edition, revised and enlarged], Pergamon Press, Oxford, 134-135 (1965).